A Simple Model for the Interference Between Event-Based Control Loops Using a Shared Medium

Henningsson, Toivo; Cervin, Anton

2010

A Simple Model for the Interference Between Event-Based Control Loops Using a Shared Medium

Toivo Henningsson and Anton Cervin

***Abstract*— Traditionally, control loops are closed using periodic sensing and actuation. When communication resources are scarce, much may be gained by instead transmitting only when something important has happened in the loop. However, there are no known closed form solutions to this kind of control problem. This paper presents a simple model of the interference between event-based control loops caused by sharing a common medium, based on approximating the behavior of all loops except one foreground loop. The stationary state distribution can be computed at low computational cost using mostly standard linear time-invariant system theory (applied in the spatial dimension). Control laws are optimized to minimize state variance using the limited communication resources. Comparison to Monte Carlo simulations of a full model shows the simple model to be remarkably accurate. The model is applied to investigate how the performance of N control loops sharing a common Carrier Sense Multiple Access channel approaches the ideal case of aperiodic control as the number of loops grows.**

I. Introduction

Event-based control holds the promise of better control performance and lower resource consumption compared to standard sampled-data control. In their seminal paper on event-based control, Åström and Bernhardsson (Å&B) [1] showed that, for an integrator process driven by white noise, event-triggered control requires only one third of the number of samples to achieve the same output variance as periodic, time-triggered control. However, the reduction comes at the cost of more irregular events. In fact, Å&B's *aperiodic* controller would require infinite bandwidth to be implemented in a networked control setting.

Aiming for implementable controllers, we have previously proposed the concept of *sporadic control* [6], where a minimum inter-event time T is enforced. The parameter T can be used to model that the communication channel stays busy for some time when a packet is transmitted.

This paper explores how the ideal performance of Å&B can be approached by letting N sporadic control loops share a communication medium with limited bandwidth. As the number of loops grows, it is expected that the medium can be used more and more efficiently, essentially transforming the sporadic constraint into a constraint on the average communication rate.

A major theoretical challenge in event-based control of stochastic systems is to find the stationary probability distribution of the state. For low-order systems, gridding of the state-space may be used, but this quickly becomes infeasible for higher-order systems. In a previous study [2], we used Monte Carlo simulations to numerically evaluate the performance for a modest number of sporadic controllers using a shared medium.

By contrast, in the current paper we derive a simple model that allows rapid evaluation of the performance, even as the number of loops becomes large. The control loops are partitioned into one *foreground loop*, and $N-1$ *background loops*. Only the state probability distribution of the foreground loop and the discrete state of the medium are modelled in detail. When the resulting problem has been solved, key model parameters are matched to make the behavior of the foreground and background loops appear equal.

Comparing with results from Monte Carlo simulations of the full system model, it is seen that the simple model is remarkably accurate in predicting the behavior of the full system, given its simplicity. The agreement becomes better as N grows, and, as N becomes very large, the ideal performance of Å&B is approached.

The medium access policy assumed in the paper is Carrier Sense Multiple Access (CSMA) with random, delay-free arbitration if several nodes attempt to transmit at the same time. The network is hence collision free—this is a key assumption for our results to hold. It is well known that the performance of ALOHA/CSMA with collisions and retransmissions breaks down when utilization approaches 1, e.g., [10], [7]. Collisions are highly relevant for wireless sensor/actuator networks and will be studied in future papers.

Related Work

Rabi and Johansson [8] analyzed how packet loss impacts the performance of event-triggered control loops. The analysis was done for a single networked loop, assuming that the loss rate was independent of the event-triggering threshold of the controller.

Event-triggered state estimation or control of higher-order systems has been studied by Cogill [5], [4], however not in the context of several competing control loops.

In all the works mentioned so far, the events are triggered by fixed thresholds in the state space. Alternative ways to trigger event-based controllers are proposed in [9], [11].

Outline

The rest of the paper is laid out as follows: Section II presents the system model and the optimal control problem. The equations for the stationary state distribution are derived in Section III and solved in Section IV, by reducing the

This work was supported by the Swedish Research Council, , ELLIIT, and EU/FP7/ArtistDesign.

T. Henningsson and A. Cervin are with the Department of Automatic Control LTH, Lund University, Box 118, SE-221 00 Lund, Sweden. Email: toivo.henningsson@control.lth.se

linear problem from infinite dimension to a small finite dimension that can be solved efficiently. Model parameters are adjusted in Section V to match key parameters between the foreground loop and the background loops. The influence of the packet length distribution is investigated in Section VI. Results and comparison to other models are presented in Section VII and possible directions for future work are discussed in section VIII. Conclusions are given in Section IX.

II. Problem Formulation

This section presents the system model, which includes the foreground loop and medium state, the conditions to match the foreground and background loops, and the optimal control problem that we want to solve.

A. System Model

The process controlled in the foreground loop is modelled as an integrator disturbed by white noise according to

$$dy = udt + \sigma dw, \tag{1}$$

where w is a Wiener process with unit incremental variance. The control signal u will be zero except when the foreground loop is able to generate a control event, at which time it will contain a Dirac impulse.

The control law is simple: whenever $|y| \geq r$ for some threshold r, the controller tries to take the channel and transmit a new packet. If it succeeds, the state y is reset to zero immediately[1].

The CSMA channel model is summarized in Fig. 1:

- Whenever the channel is Available, anyone may transmit, causing a transition into the Busy state. The foreground loop will do so when the integrator state reaches the threshold $|y| \geq r$; the background loops will do so at an expected rate λ_b.
- The transmission of a packet takes an expected time $T = \lambda_p^{-1}$. A new packet may then be initiated immediately, or the channel will become available, which will happen at a rate $\lambda_a \leq \lambda_p$ when $|y| < r$.
- If several transmitters are contending for the channel when it is released, one is picked at random. The foreground loop will be able to gain the channel in the Busy state at a rate $\lambda_{\text{prio}} \leq \lambda_p - \lambda_a$ when it wants to (i.e., when $|y| \geq r$).

The state of the system is thus $(y, k) \in \mathbb{R} \times \mathbb{Z}_n$ ($n = 2$ in this case), where k is the state of the channel, so the stationary probability density function (pdf) $f(y)$ and probability flow in the y direction $\varphi(y)$ are

$$f(y) = \begin{pmatrix} f_a(y) \\ f_b(y) \end{pmatrix}, \qquad \varphi(y) = \begin{pmatrix} \varphi_a(y) \\ \varphi_b(y) \end{pmatrix}.$$

The control law imposes the linear constraints

$$f_a(y) = 0 \ \forall |y| \geq r, \qquad \varphi(0) = \begin{pmatrix} 0 \\ \varphi_{\text{fg}} \end{pmatrix},$$

[1]It is trivial to account for a fixed delay in the control action, see [3].

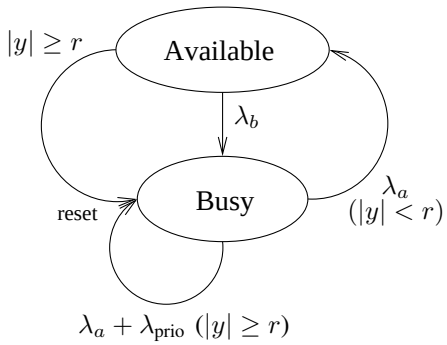

Fig. 1. Continuous-time Markov chain model of the channel state dynamics under CSMA. The dynamics depends on the integrator state y: the reset transitions are triggered only when $|y| \geq r$; when $|y| < r$ there is instead a transition to the Available state.

where φ_{fg} is the rate of reset, since the channel never stays available when $|y| \geq r$, and all resets cause inflow into the Busy state at $y = 0$.

When $|y| < r$, the channel state will evolve according to

$$\begin{pmatrix} \dot{p}_a \\ \dot{p}_b \end{pmatrix} = \begin{pmatrix} -\lambda_b & \lambda_a \\ \lambda_b & -\lambda_a \end{pmatrix} \begin{pmatrix} p_a \\ p_b \end{pmatrix},$$

where p_a and p_b are the probabilities to be in the Available and Busy states respectively. When $|y| \geq r$, the channel state will evolve according to

$$\dot{p}_b = -(\lambda_a + \lambda_{\text{prio}}) p_b;$$

the leakage corresponds to the rate of reset triggered from the Busy state.

B. Matching Conditions

We must require the foreground packet rate φ_{fg} to be a proportional share of the total packet rate $N f_u = \lambda_p p_{\text{b}}$, i.e.

$$\lambda_p p_{\text{b}} = N \varphi_{\text{fg}}. \tag{2}$$

To model equal prioritization of all loops, we demand that in the Busy state with $|y| \geq r$, the intensity to gain the channel is the total packet rate λ_p divided by the expected number of loops waiting to gain the channel, i.e.

$$\lambda_{\text{outside}} = \lambda_a + \lambda_{\text{prio}} = \frac{\lambda_p}{1 + (N-1) p_{\text{outside|b}}}. \tag{3}$$

Finally, we choose the clearing rate λ_a according to

$$\lambda_a = \lambda_p - \lambda_b, \tag{4}$$

meaning that the average rate of background packets is λ_b in the Busy state as well as in the Available state.

C. Optimal Control

The design objective is to choose an optimal threshold $r = r^*$ to minimize the state variance

$$J_y = \mathrm{E}(y^2)$$

for each loop. We may also want to trade some increase in J_y to decrease the average event rate f_u of each loop. In the Å&B case, the tradeoff is given by (see [1])

$$J_y = \tfrac{1}{6} \sigma^2 f_u^{-1} = \tfrac{1}{6} r^2. \tag{5}$$

III. The Stationary Distribution Problem

We consider now the general case of simultaneous evolution of an integrator state according to (1) (with $u = 0$) and a continuous time Markov chain. The state of the system is $(y, k) \in \mathbb{R} \times \mathbb{Z}_n$, where k is the state of the Markov chain. The pdf over the state is $f : \mathbb{R} \mapsto \mathbb{R}^n$.

A. The Spatial Dynamics

The Fokker-Planck equation for the pdf f under the Brownian motion (1) with $u = 0$ is

$$\dot{f}(y) = \tfrac{1}{2}\sigma^2 f''(y) = -\varphi'(y),$$

where $\dot{f}$ and f' are the derivatives with respect to time and integrator state y respectively, and $\varphi(y)$ is the flow of probability in the y direction. We may thus take $\varphi(y)$ to be $\varphi(y) = -\frac{1}{2}\sigma^2 f'(y)$. Simultaneously, the Markov chain state k evolves by the transition intensity matrix A_m as

$$\dot{f} = A_m f.$$

Summing the probability flows from the integrator drift and the Markov chain gives the combined dynamics

$$\dot{f}(y) = \tfrac{1}{2}\sigma^2 f''(y) + A_m f.$$

Assuming stationarity, $\dot{f} = 0$ now gives the spatial dynamics

$$f''(y) + \frac{2}{\sigma^2} A_m f = \mathcal{D} f = 0, \tag{6}$$

which can also be expressed in state space form as

$$x'(y) = \begin{pmatrix} 0 & -\frac{2}{\sigma^2} A_m \\ I & 0 \end{pmatrix} x(y), \qquad x(y) = \begin{pmatrix} f'(y) \\ f(y) \end{pmatrix}.$$

B. Moments

Aside from the actual stationary pdf $f(y)$, we will also need moments such as marginal probability over the Markov chain states $F(0)$ and state variance V, according to

$$F(0) = \int_0^\infty f(y)dy, \quad V = \int_0^\infty y^2 \mathbf{1}^T f(y)dy.$$

Since the model is symmetric with respect to the origin, we consider f to be defined only over $y \geq 0$; the extension to the non-symmetric case is straightforward. The easiest way to find these moments is to work them into the spatial dynamics.

The moments can be computed from

$$\begin{pmatrix} F(y) \\ F_1(y) \\ F_2(y) \end{pmatrix} = \int_y^\infty \begin{pmatrix} f(y) \\ \mathbf{1}^T F(y) \\ F_1(y) \end{pmatrix} dy, \tag{7}$$

where we collect individual integrals for the zeroth moment, but sum over the Markov chain states for higher moments to reduce the computational complexity. The variance is found as $V = 2F_2(0)$ by partial integration twice to eliminate the factor y^2 in the integrand.

Combining (6) and (7) gives the extended dynamics

$$x_e'(y) = \underbrace{\begin{pmatrix} 0 & -\frac{2}{\sigma^2} A_m & & & \\ I & 0 & & & \\ & -I & 0 & & \\ & & -\mathbf{1}^T & 0 & \\ & & & -1 & 0 \end{pmatrix}}_{A_{\text{full}}} \underbrace{\begin{pmatrix} f'(y) \\ f(y) \\ F(y) \\ F_1(y) \\ F_2(y) \end{pmatrix}}_{x_e(y)}, \tag{8}$$

with boundary conditions $x \to 0$ as $|y| \to \infty$. We see that (8) has a triangular structure such that the the integrated densities F_i depend on f and f' but not vice versa.

C. Causal/Anticausal Decomposition

The operator $\mathcal{D}$ of (6) can be factored into a causal part $\mathcal{D}_-$ and an anticausal part $\mathcal{D}_+$ according to

$$\mathcal{D} = \frac{d^2}{dy^2} + \frac{2}{\sigma^2} A_m f \; = \mathcal{D}_+ \mathcal{D}_- \qquad\qquad = \mathcal{D}_- \mathcal{D}_+,$$

$$\mathcal{D}_+ = \frac{d}{dy} - A_+, \quad \mathcal{D}_- = \frac{d}{dy} + A_+, \quad A_+ = \sqrt{-\frac{2}{\sigma^2} A_m}.$$

The square root exists since A_m must have a full zero eigenspace, or the temporal dynamics $\dot{p} = A_m p$ would have an unbounded solution. Since A_m has all eigenvalues in the left half plane, A_+ will have eigenvalues λ in the sector $\Re(\lambda) \geq |\Im(\lambda)|$. The poles of the spatial dynamics (6) will be the eigenvalues of $\pm A_+$, thus satisfying $|\Re(\lambda)| \geq |\Im(\lambda)|$.

IV. Solving the Spatial Dynamics

The stationary density $f(y)$ is the solution to a set of linear equations composed of the spatial dynamics (8) which is piecewise constant in y, additional linear conditions specified in the model, and the normalization condition $\int f(y)dy = 1$. By solving (8) over an interval, we can eliminate the interior values of $x_e(y)$, leaving a low-dimensional set of linear equations to solve for $f(y)$. The moments and interior values of $f(y)$ can then be reconstructed.

The extended dynamics (8) can be solved using standard linear time invariant system theory. We must be careful since the dynamics is reversible, consisting of matching stable and antistable, or rather causal and anticausal parts.

A. Bounded Intervals

We want to solve (8) over an interval $[y_0, y_1]$. LTI system theory gives that this relation can be expressed as

$$x_e(y_1) = e^{A_{\text{full}} \Delta y} x_e(y_0), \qquad \Delta y = y_1 - y_0. \tag{9}$$

This formulation may, however, be very ill conditioned.

Premultiplying (9) by the scaling matrix $(e^{A_{\text{full}} \Delta y} + I)^{-1}$ gives the equivalent relation

$$h\big(-\tfrac{1}{2} A_{\text{full}} \Delta y\big) x_e(y_1) = h\big(\tfrac{1}{2} A_{\text{full}} \Delta y\big) x_e(y_0), \tag{10}$$

where the analytical function h is given by

$$h(At) = \big(e^{At} + e^{-At}\big)^{-1} e^{At} = \tfrac{1}{2}\big(I + \tanh(At)\big).$$

This formulation will in general be much better conditioned than (9). [2]

The function $h(\pm At)$ can be evaluated efficiently through the doubling recursion

$$h(2At) = \Big(h(At)^2 + h(-At)^2\Big)^{-1} h(At)^2;$$

$h(\pm 2^{-n}At)$ is first evaluated for some suitable n such that $e^{\pm 2^{-n}At}$ is reasonably conditioned, $h(\pm At)$ is then found in a modest number of steps. If A is first put on Schur form $h(At)$ will be triangular, and all necessary matrix inversions can be done efficiently through back substitution.

B. Semiinfinite Intervals

When solving (6) over a semiinfinite interval $[y_0, \infty)$ we must insist that A_m has some leakage (thus having eigenvalues strictly in the left half plane) to be able to satisfy the boundary conditions that $f \to 0$ as $y \to \infty$. The solution of (6) is then

$$f(y) = e^{-A_+(y-y_0)} f(y_0), \tag{11}$$

implying the equivalent boundary conditions at $y = y_0$

$$f'(y_0) + A_+ f(y_0) = 0.$$

The integrals F_i can be found by direct integration of (11).

C. Interpolating the Probability Density Function

Given the boundary conditions $x(y_0), x(y_1)$, the pdf $f(y)$ can be interpolated according to

$$\mathcal{D}_-\mathcal{D}_+ f = \mathcal{D}_- g = 0, \quad \mathcal{D}_+ f = g.$$

First, g is solved for in the causal direction, with initial conditions given by

$$g(y_0) = (\mathcal{D}_+ f)(y_0) = f'(y_0) - A f(y_0).$$

Then, f is solved for in the anticausal direction, with initial conditions $f(y_1)$ and input $g(y)$. With semiinfinite intervals, it is enough to solve outwards from the finite endpoint.

V. Matching the Loops

Now that we can solve a problem instance given specific model parameters, we want to adjust the model parameters λ_a, λ_b and λ_{prio} so that all N loops behave the same, i.e. the matching conditions (2), (3) and (4) are fulfilled. The condition (4) is simply realized by parametrizing λ_a in λ_b, which implies the restriction $\lambda_b \in [0, \lambda_p]$.

Suppose that we know λ_b, λ_a and want to find λ_{prio} to satisfy (2). The spatial dynamics inside the threshold is then known, and the corresponding linear relations can be used. The spatial dynamics for the outside gives that

$$p_{\text{b,outside}} = \frac{f_b(r)^2}{-f_b'(r)},$$

since $f_b(y)$ is a decaying exponential function for $y \geq r$. Inserting this expression into (2) gives the relation

$$\frac{f_b(r)^2}{-f_b'(r)} + \underbrace{p_{\text{b,inside}} - \frac{N}{\lambda_p}\varphi_{\text{fg}}}_{\text{linear in } (f_b(r),\, f_b'(r))} = 0.$$

Fixing e.g. $f_b'(r)$ we get a quadratic equation in $f_b(r)$, with one positive solution. We can now solve for λ_{outside} from

$$f_b'(r) = -\sqrt{\frac{2}{\sigma^2}\lambda_{\text{outside}}}\, f_b(r).$$

When all parameters are known, the solution is finally normalized to unit total probability. We can normalize afterwards, since all other conditions on $f(y)$ are purely linear.

To match also the priority according to (3), we can use i.e. secant search over λ_b. We know that $\lambda_{\text{outside}} \in [\lambda_a, \lambda_p]$; a secant search over λ_b to satisfy (2) for each of these fixed endpoints gives a suitable starting interval for the priority matching. Sometimes there is no $\lambda_b \in [0, \lambda_p]$ that satisfies (2) with $\lambda_{\text{outside}} = \lambda_p$; we then use $\lambda_b = \lambda_p$ as the right endpoint of the search instead.

VI. Correction for the Waiting Time Distribution

So far, we have assumed that each packet occupies the medium for an exponentially distributed waiting time, which allows to use a simple Markov chain model for the channel state. We will now investigate the influence of the waiting time distribution on the state variance $V_y(t) = \mathrm{E}(y(t)^2)$ to derive a first order correction to the state cost J_y.

By the dynamics (1), $V_y(t)$ evolves between events as

$$V_y(t) = \sigma^2 t + V_y(0);$$

during a waiting time τ this gives the accumulated variance

$$V_{\text{acc}}(\tau) = \int_0^\tau V_y(t)dt = \tfrac{1}{2}\sigma^2\tau^2 + \tau V_y(0).$$

The waiting time of one packet is $\tau, \mathrm{E}(\tau) = T$, which gives the expected final and accumulated variances

$$\begin{aligned}\mathrm{E}\big(V_y(\tau)\big) &= \sigma^2 T + V_y(0),\\ \mathrm{E}\big(V_{\text{acc}}(\tau)\big) &= \tfrac{1}{2}\sigma^2\big(T^2 + \mathrm{V}(\tau)\big) + T V_y(0).\end{aligned}$$

Keeping T fixed, the final state variance when the packet is completed stays fixed as well. The accumulated variance, however, depends also on the variance $\mathrm{V}(\tau)$. Compared to a fixed waiting time, an exponential waiting time will make V_{acc} bigger by the term

$$\Delta V_{\text{acc}} = \tfrac{1}{2}\sigma^2\,\mathrm{V}(\tau) = \tfrac{1}{2}\sigma^2 T^2.$$

Since the total packet rate is $N f_u = \lambda_p p_{\text{b}}, \lambda_p = T^{-1}$, the state cost J_y with exponential waiting times is bigger by

$$\Delta J_y = N f_u \Delta V_{\text{acc}} = \tfrac{1}{2}\sigma^2 p_b \lambda_p^{-1}. \tag{12}$$

[2] Half of the eigenvalues of $h(At)$ will satisfy $|\lambda_+| \in [0.5, 1.07]$, each corresponding to an eigenvalue $|\lambda_-| \in [0, 0.5]$ of $h(-At)$ with the same eigenspace, and vice versa for the other half of the eigenvalues. (This can be seen by looking at the behavior of $\log(|h(at)|)$ along the boundary line $at = (1 \pm i)t$); $\log(|h(at)|)$ is a harmonic function on $|\Re(at)| \geq |\Im(at)|$).

VII. Results

All results are derived with the parameters $\sigma = 1$ and $\lambda_p = N$. The latter means that the network bandwidth scales in proportion to the number of loops. This scaling is convenient since it makes the Å&B performance independent of N. The relative state variance and packet rate of the control schemes are unaffected by the choice of σ and λ_p since the integrator has no time constant.

We will compare the following models:

- Å&B's ideal, aperiodic controller, with $r = f_u = 1$ and $J_y = \frac{1}{6}$ [1]. This is a lower bound on the achievable performance.
- A Monte Carlo simulation model with N sporadic control loops competing for the network under CSMA with random arbitration [2]. The transmission time of each packet is assumed fixed and equal to $T = N^{-1}$. Via bisection search over r, the optimal performance has been found for $N \in \{1, 2, 3, 5, 10, 20, 45, 100, 200\}$. The time granularity of the model was $N^{-1}10^{-3}$ and each simulation ran for 10^8 time steps.
- The simple model proposed in this paper. In the model, the transmission times are exponentially distributed with mean $T = N^{-1} = \lambda_p^{-1}$; the cost correction (12) has been subtracted from J_y to predict the state variance with fixed rather than exponential packet times.

A. Probability Densities

Fig. 2 shows the stationary pdf $f(y)$ obtained by the simple model with $N = 10$ loops. The optimal threshold $r = r^*$ is chosen to minimize state variance J_y. The pdf of Å&B is shown for reference.

We see that, just as in the Å&B case, the pdf of the integrator state y varies linearly inside the threshold, with a break in the origin because of inflow from reset. In the simple model however, the inflow goes into the Busy state, while the outflow from reset is divided between the Available state at the threshold and the Busy state outside the threshold.

The resulting difference between the pdf:s of the Å&B case and the simple model is that the latter includes an exponential tail outside the threshold r, while the loop is waiting to gain access to the channel.

B. Threshold Dependence

Figs. 3 and 4 show the dependence of state cost J_y and packet rate f_u on threshold r, with $N = 10$ and $N = 10^5$ loops. Monte Carlo (MC) results with $N = 10$ loops and Å&B results are shown for comparison.

We see that the state cost J_y has a minimum around $r = 1$, while f_u drops monotonically with the threshold. By using a threshold $r > r^*$, it is possible to trade a decreased packet rate f_u for an increased state cost J_y; nothing is gained by using $r < r^*$. The simple model is remarkably accurate in predicting the Monte Carlo results for the full model, given the radically lower computation complexity.

As the threshold r grows, all curves tend to the Å&B case, which serves as a lower bound on J_y and an upper bound on f_u. For $N = 10$ loops, the convergence is gradual. For

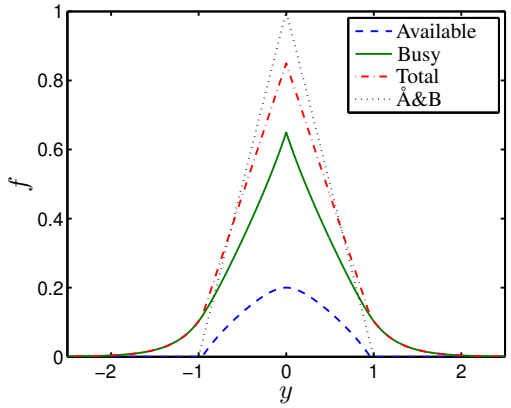

Fig. 2. The stationary pdf $f(y)$ according to the simple model with $N = 10$ loops and optimal threshold $r = 0.96$. The Å&B pdf is shown for comparison.

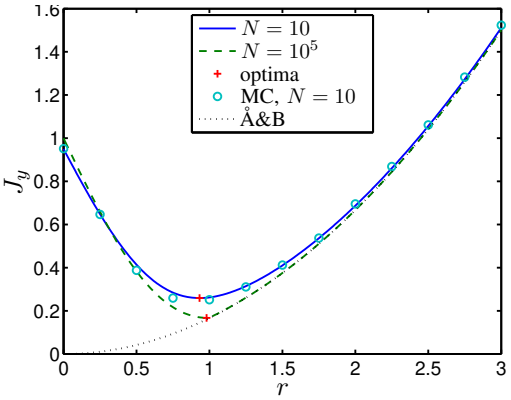

Fig. 3. State cost J_y as a function of threshold r according to the simple model for different number of loops N, along with the Å&B case and Monte Carlo results for the full model. The Å&B case serves as a lower bound for both $N = 10$ and $N = 10^5$, with the two essentially coinciding in the latter case beyond the optimum $r = r^*$.

$N = 10^5$, we can distinguish two domains: when $r \geq r^*$, J_y and f_u essentially coincide with Å&B; when $r \leq r^*$, f_u lies at the channel capacity while the state cost J_y deteriorates as the threshold r decreases.

It thus seems that for large N, performance follows the Å&B case as soon as the necessary average packet rate f_u lies within the peak packet rate of the channel; the minimal state cost J_y^* is achieved at this break point.

C. Dependence on the Number of Loops

The threshold r was optimized using golden section search to minimize state cost J_y as a function of N. Fig. 5 shows optimal state cost J_y, packet rate f_u and threshold r as N varies from 1 to 10^5 for the simple model, along with full model Monte Carlo and Å&B results for comparison.

We see that as N increases, J_y drops from about 0.4 towards the Å&B case of $J_y = \frac{1}{6}$. The simple model is slightly optimistic about J_y for $N = 1$, and slightly pessimistic for $N \geq 2$. Convergence to the Å&B case is very close at $N = 10^3$.

The rise in packet rate f_u with N shows a similar pattern

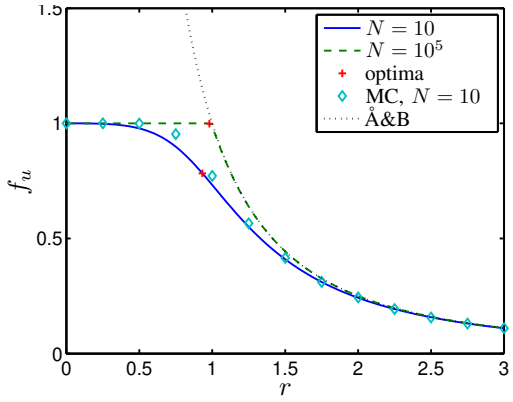

Fig. 4. Packet rate f_u as a function of threshold r according to the simple model for different number of loops N, along with the Å&B case and Monte Carlo results for the full model. The Å&B case serves as an upper bound for both $N = 10$ and $N = 10^5$, with the two essentially coinciding in the latter case beyond the optimum $r = r^*$.

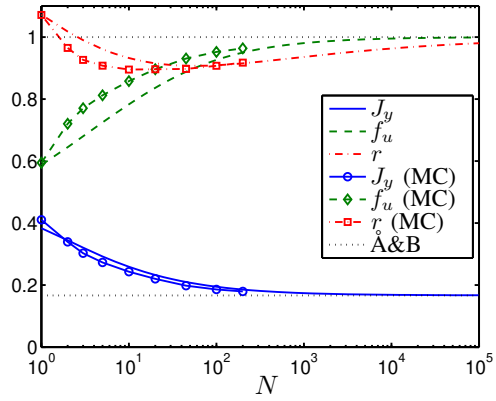

Fig. 5. Optimal state cost J_y, packet rate f_u, and threshold r as a function of number of loops N. Results are shown for the simple model, full model Monte Carlo simulations, and the aperiodic Å&B case (for which $J_y = \frac{1}{6}, f_u = r = 1$).

to the drop in J_y; this rise is in fact necessary to bring J_y down since the Å&B performance (5) lower bounds $J_y(f_u)$. In accordance, the slightly lower state cost J_y of the full model Monte Carlo results is accompanied by a higher packet rate f_u, realized by a quicker drop in threshold r.

VIII. Future Work

A main direction for continued research is to apply the same kind of modelling developed in this paper to other channel models, such as with partial and full collisions. It is then probably better to trigger control events at a bounded intensity once the threshold is crossed. Points that deserve further study include

- How should the shared medium best be utilized when collisions lead to packet drop?
- How does a partial collisions model transition from CSMA behavior to full collision behavior as time to detect that the channel is busy changes?
- Can the model be extended to general first order process dynamics, or to processes with higher state dimension?

IX. Conclusion

Event based control offers the promise to better utilize limited communication resources than traditional periodic control. The potential benefit increases with the number of control loops sharing the same medium, as they may be able to trade use of the communication channel between each other to be able to gain access when it is most needed. The potential for interference, however, also increases; the question is which of the effects dominates.

This paper presents a simple model for the interaction between N event based control loops sharing a common medium in the form of a CSMA channel. The model includes the medium and a single foreground loop, approximating the behavior of the other (background) loops. The resulting model can be evaluated with little computational resources, independent of N.

Comparison to Monte Carlo simulations of the simultaneous evolution of all loops shows that the simple model predicts the behavior of the full model with remarkable accuracy, given its simplicity. As the number of loops increases, they are able to share the medium more and more efficiently, making the sporadic channel constraint appear more and more like an average capacity constraint, resulting in significantly improved performance .

Acknowledgment

The authors would like to thank M. Rabi for fruitful discussions leading up to the model used in this paper. This work has been supported by the Swedish Research Council, ELLIIT, and EU/FP7/ArtistDesign.

References

[1] K. J. Åström and B. Bernhardsson. Comparison of periodic and event based sampling for first-order stochastic systems. In *Preprints of the 14th World Congress of IFAC*, Beijing, P.R. China, 1999.

[2] A. Cervin and T. Henningsson. Scheduling of event-triggered controllers on a shared network. In *Proc. 47th IEEE Conference on Decision and Control*, Cancun, Mexico, Dec. 2008.

[3] A. Cervin and E. Johannesson. Sporadic control of scalar systems with delay, jitter and measurement noise. In *Proc. 17th IFAC World Congress*, Seoul, Korea, July 2008.

[4] R. Cogill. Event-based control using quadratic approximate value functions. In *Proc. IEEE Conference on Decision and Control*, Shanghai, P.R. China, 2009.

[5] R. Cogill, S. Lall, and J. P. Hespanha. A constant factor approximation algorithm for event-based sampling. In *Proc. Allerton Conference on Communication, Control, And Computing*, 2006.

[6] T. Henningsson, E. Johannesson, and A. Cervin. Sporadic event-based control of first-order linear stochastic systems. *Automatica*, 44(11):2890–2895, Nov. 2008.

[7] P. R. Jelenković and J. Tan. Is ALOHA causing power law delays? In *Managing Traffic Performance in Converged Networks*, volume 4516 of *Lecture Notes in Computer Science*. Springer, 2007.

[8] M. Rabi and K. H. Johansson. Scheduling packets for event-triggered control. In *Proc. 2009 European Control Conference*, Budapest, Hungary, Aug. 2009.

[9] P. Tabuada. Event-triggered real-time scheduling of stabilizing control tasks. *IEEE Transactions on Automatic Control*, 52(9):1680–1685, 2007.

[10] F. A. Tobagi and V. B. Hunt. Performance analysis of carrier sense multiple access with collision detection. *Computer Networks*, 4(5):245–259, 1980.

[11] X. Wang and M. Lemmon. Self-triggered feedback control systems with finite-gain $\mathcal{L}_2$ stability. *IEEE Transactions on Automatic Control*, 45(3):452–467, 2009.